J Neurophysiol 111: 2138–2149, 2014.
First published February 26, 2014; doi:10.1152/jn.00802.2013.

Monkeys time their pauses of movement and not their movement-kinematics during a synchronization-continuation rhythmic task

Sophie Donnet,[1] Ramon Bartolo,[2] José Maria Fernandes,[3] João Paulo Silva Cunha,[4] Luis Prado,[2] and Hugo Merchant[2]

[1]*Unité Mathématiques et Informatique Appliquées, Institut National de la Recherche Agronomique, Paris, France;* [2]*Instituto de Neurobiología, Universidad Nacional Autónoma de México, Querétaro, México;* [3]*Instituto de Engenharia Electrónica e Telemática de Aveiro/Departamento de Electrónica, Telecomunicações e Informática, Universidade de Aveiro, Aveiro, Portugal; and* [4]*Department of Electrical and Computer Engineering, Faculty of Engineering, University of Porto/Instituto de Engenharia de Sistemas e Computadores Tecnologia e Ciência, Porto, Portugal*

Submitted 8 November 2013; accepted in final form 24 February 2014

Donnet S, Bartolo R, Fernandes JM, Cunha JP, Prado L, Merchant H. Monkeys time their pauses of movement and not their movement-kinematics during a synchronization-continuation rhythmic task. *J Neurophysiol* 111: 2138–2149, 2014. First published February 26, 2014; doi:10.1152/jn.00802.2013.—A critical question in tapping behavior is to understand whether the temporal control is exerted on the duration and trajectory of the downward-upward hand movement or on the pause between hand movements. In the present study, we determined the duration of both the movement execution and pauses of monkeys performing a synchronization-continuation task (SCT), using the speed profile of their tapping behavior. We found a linear increase in the variance of pause-duration as a function of interval, while the variance of the motor implementation was relatively constant across intervals. In fact, 96% of the variability of the duration of a complete tapping cycle (pause + movement) was due to the variability of the pause duration. In addition, we performed a Bayesian model selection to determine the effect of interval duration (450–1,000 ms), serial-order (1–6 produced intervals), task phase (sensory cued or internally driven), and marker modality (auditory or visual) on the duration of the movement-pause and tapping movement. The results showed that the most important parameter used to successfully perform the SCT was the control of the pause duration. We also found that the kinematics of the tapping movements was concordant with a stereotyped ballistic control of the hand pressing the push-button. The present findings support the idea that monkeys used an explicit timing strategy to perform the SCT, where a dedicated timing mechanism controlled the duration of the pauses of movement, while also triggered the execution of fixed movements across each interval of the rhythmic sequence.

interval timing; time production; Rhesus monkey; movement kinematics; model testing

INTERVAL TIMING IN THE SCALE of milliseconds is a substrate for many complex activities, including the perception and production of speech, music, and dance (Diehl et al. 2004; Janata and Grafton 2003; Merchant et al. 2013a; Phillips-Silver and Trainor 2007), as well as the estimation of the time that remains before the occurrence of an important event during sport performance (Merchant and Georgopoulos 2006; Merchant et al. 2009). The ability to capture and interpret the beats in a rhythmic pattern allows people to move and dance in time to music (Merchant and Honing 2014; Phillips-Silver and Trainor 2007). Music and dance, then, are behaviors that depend on intricate loops of perception and action, where temporal processing can be involved during the synchronization of movements with sensory information or during the internal generation of movement sequences (Repp and Su 2013). The synchronization-continuation task (SCT) is a simplified version of these processes that has been a backbone tool in the timing literature (Repp 2005; Wing 2002). In this task subjects perform tapping movements that are initially guided by a sensory metronome of isochronous intervals, and then they continue tapping without the advantage of a sensory cue. In this regard, our laboratory has shown that different populations of neurons in the medial premotor cortex (MPC) of the primate encode the elapsed and the remaining time for an action during the performance of the SCT (Merchant et al. 2011). This study suggests that the rhythmic nature of the SCT may depend on the close interaction between these two cell populations (Merchant et al. 2011). In addition, MPC cells are tuned to the duration of produced intervals during this rhythmic tapping task. In fact, the same population of neurons is able to simultaneously encode the ordinal structure of a sequence of rhythmic movements and a wide range of durations in the range of hundreds of milliseconds (Merchant et al. 2013b). These findings suggest that MPC uses interval tuning as an abstract representation of the passage of time, where a cell population signal works as the notes of a musical score to represent both the duration of the produced interval and the rank order of the interval that is executed in the learned SCT sequence (Merchant et al. 2013b; Perez et al. 2013). However, since the MPC is a motor area connected with the spinal cord (Dum and Strick 1996), it is important to determine whether or not the tapping movements showed differences across the durations and the sequential order of the tested SCT that could explain the described tuning responses in motor terms. Furthermore, it is crucial to demonstrate that the monkeys performed a phasic tapping task instead of a continuous cyclic movement that could change the rules of temporal processing from an explicit to an implicit timing behavior, as it has been reported previously in a circle drawing task (Merchant et al. 2008a; Robertson et al. 1992; Zelaznik et al. 2002, 2005). In the present paper, we determined the effect of interval duration, serial structure, the sensory-cued or internal-driven nature of rhythmic movements (synchronization or continuation phase),

Address for reprint requests and other correspondence: H. Merchant, Instituto de Neurobiología, UNAM campus Juriquilla, Cognitive Neuroscience, Boulevard Juriquilla, No. 3001, Querétaro 76230, Mexico (e-mail: hugomerchant@unam.mx).

and the stimulus modality used as an interval marker on the cyclic control of the hand movement during the SCT execution by trained monkeys. The speed profile of the tapping movements was carried out using semiautomatic video-tracking algorithms (Fernandes et al. 2011), which allowed the identification of the beginning and end of each tapping movement, as well as the duration of the pause of movement in the trial sequence of the SCT. An initial analysis demonstrated a linear increase in the variance of pause-duration as a function of interval, while the variance of the motor implementation is relatively constant across the produce intervals. These results indicate that only the pause follows the scalar property of interval timing (Gibbon et al. 1997) and suggest that monkeys used a central timing mechanism to quantify the pause-durations (Zarco et al. 2009). Then we performed a Bayesian model selection for all possible model combinations that assessed the effect of our four independent variables (interval duration, serial-order, task phase, and marker modality) on the duration of both the pause of movement and the tapping movement. The results showed that the most important parameter used to successfully perform the SCT was the control of the pause in movement duration, with important interactions between the interval duration and the sequential order on the duration of the pause of movement. In addition, the results also indicate that the kinematics of the tapping movements were concordant with a stereotyped control of the hand pressing the push-button, which was not importantly affected by the duration of the produced intervals, the sequential structure of the task, or the modality of the interval marker. The present findings support the notion that monkeys used an explicit timing strategy to perform the SCT, where the timing mechanism controlled the duration of the pauses of movement and also triggered the execution of a similar downward-upward hand movement across each produced interval in the rhythmic sequence.

METHODS

Animals

Two male monkeys (*Macaca mulatta* 5–7 kg, referred to as M01 and M02) were used. The ages of the monkeys were 9 and 8 yr, respectively. M01 was right-handed, and M02 was left-handed. All experimental procedures with the animals were approved by the National University of Mexico Institutional Animal Care and Use Committee and conformed to the principles outlined in the Guide for Care and Use of Laboratory Animals (National Institutes of Health, publication no. 85–23, revised 1985).

Apparatus

Monkeys were seated in a primate chair in a sound-attenuated room facing a computer screen. The animals tapped on the same type of push-button with one hand, whereas their opposite arm was comfortably restrained during the task. The monkeys started each trial in the tasks by putting their working hand on a horizontal key (with infrared sensors) that was placed next to the push-button. The stimulus presentation and the collection of behavioral responses were computer-controlled by a custom-made Visual Basic program (Microsoft Visual Basic 6.0, 1998). Auditory stimuli were presented through two equidistant front speakers, and the monitor was at a distance of 57 cm from the monkeys' eyes.

SCT

Experimental task. The SCT used in this study has been described before (Merchant et al. 2011; Zarco et al. 2009). Briefly, the monkeys were required to push a button each time stimuli with a constant interstimulus interval were presented, which resulted in a stimulus-movement cycle (Fig. 1). After four consecutive synchronized movements, the stimuli were eliminated, and the monkeys continued tapping with the same interval for three additional intervals, producing six sequential intertap intervals. Liquid reward contingencies changed as a function of the trial duration, as described elsewhere (Bartolo et al. 2014; Zarco et al. 2009). Trials were separated by a variable intertrial interval (2–4 s). Trials with produced intervals below 18% of absolute error with respect to the target interval were considered correct. The target intertap intervals, defined by brief auditory (33 ms, 2,000 Hz, 65 dB) or visual (32 ms, 10 × 10 cm^2) stimuli were 450, 550, 650, 850, and 1,000 ms, and were presented in random order within a repetition.

Stimuli. The auditory stimuli were pure tones (33 ms, 2,000 Hz, 65 dB), whereas visual stimuli were 4-cm side red squares presented in the center of a computer screen for 33 ms. The frame rate of the video board (60 Hz) was accurately calibrated, and both the visual and auditory stimuli, although brief, were clearly detectable. The target intervals were 450, 550, 650, 850, and 1,000 ms and were chosen pseudorandomly within a repetition.

Timing Task Procedure

The subjects performed the SCT in the visual or auditory interval marker condition in random order in three daily sessions. In each session, five repetitions for each interval were collected. Therefore, for each interval and modality, we collected a total of 450 produced intervals [5 durations × 6 intervals (3 synchronization + 3 continuation) × 15 repetitions]. Before data collection, the monkeys were highly trained in the SCT, with a performance above 70% of correct trials (Zarco et al. 2009).

Video Recording

Video recordings were acquired using a Sony Handycam (DCR-SR45) digital video recorder. The camera was located to the right of the monkey, deviated from the monkey-monitor axis to get a better view of the hand movement (~20° for monkey M01 and ~35° for M02) with an elevation of ~40°. The distance between the camera lens and the tapping button was 90–95 cm. A contrasting visual

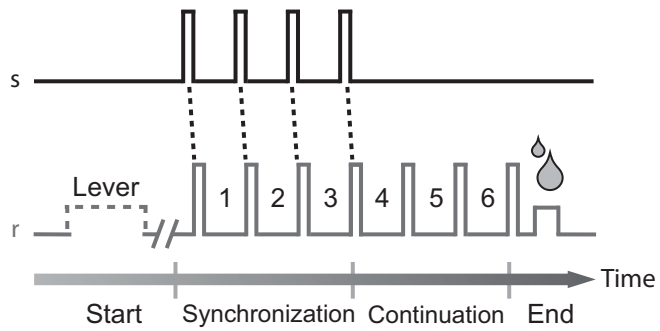

Fig. 1. Synchronization-continuation task (SCT). Monkeys were required to push a button (r; gray line) each time stimuli with a constant interstimulus interval (s; black line) were presented, which resulted in a stimulus-movement cycle. After four consecutive synchronized movements, the stimuli stopped, and the monkeys continued tapping with a similar interval for three additional intervals. Hence, six intertap intervals are generated by the monkeys in each trial. The target intervals, defined by brief auditory or visual stimuli, were 450, 550, 650, 850, and 1,000 ms and were chosen pseudorandomly within a repetition.

marker was painted on the wrist using nontoxic water-based white paint to improve movement tracking. Video was stored using MPEG-2/ACC compression under NTSC-digital standard, with a frame rate of 29.9 frames/s.

Extracting the Movement Velocity

The marker on the monkeys' hand was used to track the change in position over time during the task performance (Fig. 2*A*). After the coordinates of each frame (Fig. 2*B*) were extracted, a two-dimensional trajectory of the hand was obtained in the video reference space (see Fig. 2, *C* and *D*). Velocity was estimated based on the tracking trajectory using the norm of the difference between two consecutive positions (pixels) in the trajectory. The velocity is expressed in pixel/frame, as illustrated in Fig. 2*E*. Based on the joint observation of both trajectory and the velocity profile, the button press was identified at the first inflexion on velocity (arrow in Fig. 2*E*) after hand trajectory reaches the button (*position 3* in Fig. 2*E*).

Decomposing the Behavior

To study the behavior, we decomposed the speed profiles into trials and then into movements. In Fig. 3, *A–C*, we plotted the complete speed profiles of three particular experiments. For one particular speed profile (M01, auditory condition), we made a zoom on an arbitrarily chosen trial (Fig. 3*D*). The speed profiles were decomposed as follows. In a first step, we isolated the trials, considering that between two trials the hand stays immobile during at least 5 s. By examining each potential trial, we removed the incorrect ones: for some of them, a quick examination proved that the observed signal was in fact only the observation of noisy movements of the subject. Once the 25 correct trials had been isolated and associated to their time duration, we decomposed the speed profile of each trial into pauses and movements in the following way.

The first movement of every trial had a particular speed profile, with a significantly high peak (higher than any other peak): indeed, for this first tap, the monkey had to move his hand from the horizontal key to the push-button. The first tap occurred at some point of this first peak. The first movement was followed by a pause, corresponding to the monkey waiting for the second tap, until he started moving his hand again, for the next movement. In an ideal trial, we would count six pauses and seven movements. The last movement corresponded to the return of the monkey's hand to its original position and so was not taken into account. If the signal contained a speed peak before the first high peak identified as the beginning of the experiment, this movement would be removed from the study, since it corresponded to a noisy observation (see the arrow in Fig. 3*D* for an example).

For one particular experiment, we were not able recover the sequence of the target intervals. As a consequence, this experiment was removed from the study. For 2.2% of the remaining trials, we were not able to identify the seven movements described below, and such trials were removed from the dataset.

Statistical Analysis of Behavioral Data

In the analysis of behavioral data, three factors are susceptible to have a nonnegligible effect, namely the duration of the time interval, the type of modality (visual or auditory) and the serial order of the movement in the trial sequence (the first three being referred as "synchronization", whereas the three following ones are referred as "continuation"). To test the relevance of these three effects on the movement and the pause, we propose to use a Bayesian model selection procedure.

The work is organized as follows. A preliminary statistical analysis is performed before a finer statistical analysis. For this second analysis, we first introduce useful notations and present the various statistical models we consider. Then the concept of Bayesian model selection is quickly introduced, and, finally, the results of the model selection procedure are presented and commented. Note that the Bayesian model selection and the calculus are detailed in APPENDIX B.

An Initial Descriptive Analysis of the Data

Let $(p_i)_{i=1\ldots n}$ and $(m_i)_{i=1\ldots n}$ denote, respectively, the collection of all the pause and movement durations for all the trials and for both monkeys. The main objective of our statistical study is to understand the variability of the pause and movement durations. A first indication of this variability can be given by the following analysis. Considering

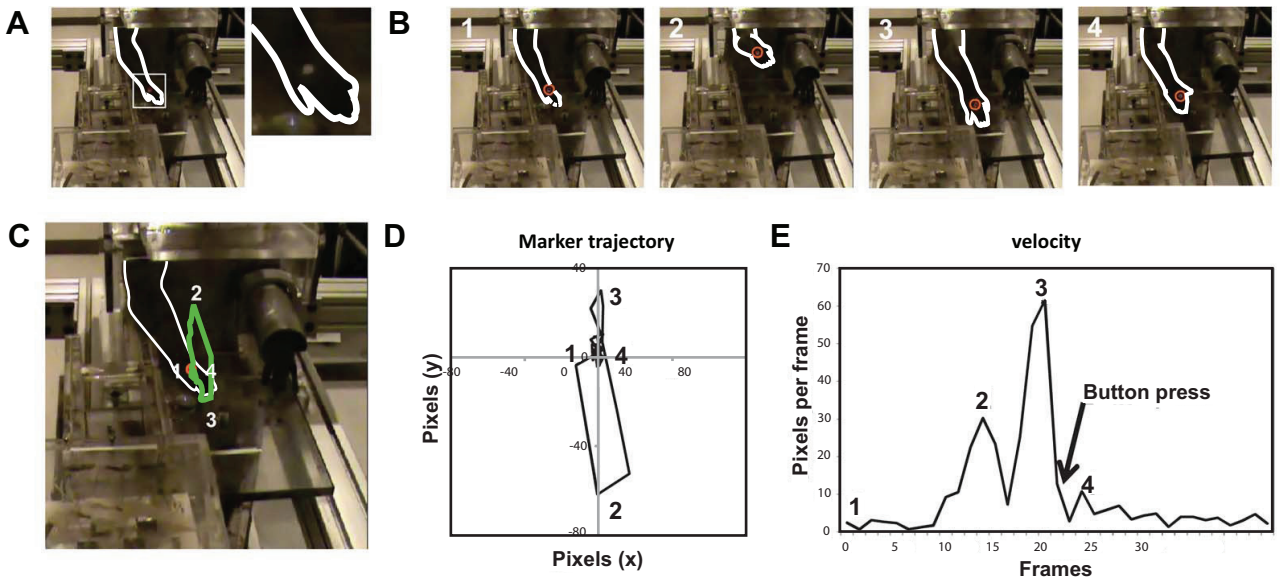

Fig. 2. Tracking the monkey's hand motion. The hand marker (circle; *A*) was identified frame by frame (*B*). The trajectory (*C*) and marker position (*D*) were extracted in coordinates relative to *position 1*. *E*: the velocity was calculated using the displacement in pixel in consecutive frame. The button-pressing event was identified in velocity profile as being the inflexion after peak in *position 3*, shown as an arrow in the graph.

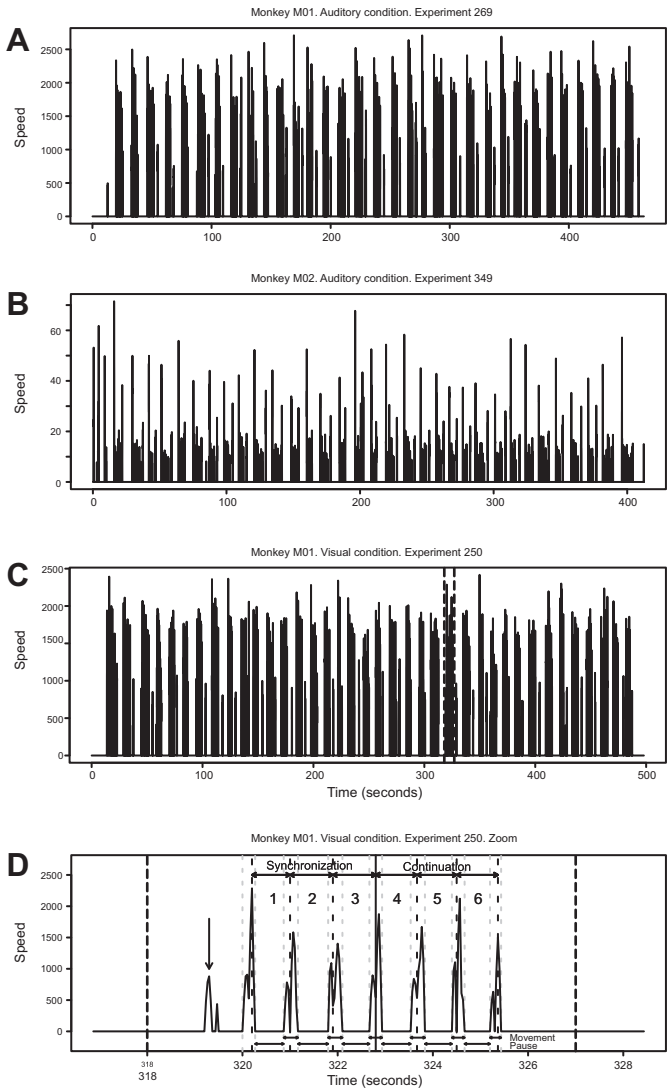

Fig. 3. Plot of three speed profiles with 25 correct trials collected during a video recording session. *A*: monkey 01, auditory condition. *B*: monkey 02, auditory condition. *C*: monkey 01, visual condition. *D*: zoom on one particular trial (delimitated by the two bold dashed lines in *C*). Dashed lines: tap instants. Arrows above the interval number: intertap durations (the first three corresponds to the synchronization phase, the three following ones are in the continuation phase). First horizontal arrows below the speed profiles: movement durations. Second horizontal arrows below the speed profiles: pause durations. Large vertical arrow: sporeous movement.

that a complete cycle (response to a given stimulus) is composed of a movement (m_i) and a pause (p_i), we decompose the variability of the duration of a complete cycle ($p_i + m_i$) using the following formulae:

$$Var(p + m) = Var(p) + Var(m) + 2Cov(m, p)$$

In our case, we obtain the following values (computed on the entire dataset):

$$Var(p + m) = 0.0395,\ Var(p) = 0.0381,\quad Var(m) = 0.0032,$$
$$Cov(m,\ p) = -0.0009$$

meaning that roughly 96% of the variability of the duration of a complete cycle ($p + m$) is due to the variability of the pause duration, the remaining being explained by a small variability of the movement (8% of the total variability) and a small negative covariation (−2.2%) between the pause and movement durations.

If we want to understand the reasons for this variability, we can (in a preliminary study) plot the probability distributions of the pause and movement durations (for all the available data), with respect to the imposed time interval. These distributions are plotted in Fig. 4. The distribution of the durations for all the time durations is in black (plain line), the other curves are for each type of time duration. Note that the probability distributions are obtained by kernel density estimation, which is an adapted version of histograms for continuous data (see Silverman 1986). We clearly see that the probability distributions of the movement durations are constant when the time duration varies, which is not the case for the pause durations. This is corroborated by Fig. 4*C*, which shows a linear increase of the pause variability as a function of the squared time interval (slope of the linear regression equal to $1.23\ 10^{-8}$), while the variance of the motor implementation is smaller and relatively constant across intervals (slope of the linear regression equal to $4.52\ 10^{-10}$). The linear correlation coefficients also support this remark $\{Cor[p, (t^s)^2] = 0.77$ and $Cor[m,(t^s)^2] = 0.49\}$.

In the next section, we propose a finer analysis of these phenomena, taking into account other factors, such as the modality (auditory or visual) and the serial order of the movement in the trial.

Complete Analysis of the Variability of the Pause and Movement Durations

Let us consider the data for one subject, submitted to three visual and three auditory experiments. Each experiment is composed of 25 trials, 1 trial corresponding to one of the 5 durations; thus each duration is repeated 5 times pseudorandomly in an experiment. Each trial corresponds to seven taps (4 in the synchronization phase and subsequently 3 in the continuation phase).

Let k denote the type of modality: $k = 1$ (respectively 2) corresponding to the auditory or visual modality. Let $i \in \{1,...,N_k\}$ denote the index of the trial, each trial corresponding to a duration t^s. We denote by j the serial order of the movement in the trial, $j \in \{1,...,6\}$. $j \in \{1,...,3\}$ corresponds to the synchronization phase, whereas $j \in \{4,...,6\}$ corresponds to the continuation phase. Let p_{ijk} (respectively m_{ijk}) be the j-th pause (respectively movement) duration for trial i and modality k. p_{ijk} and m_{ijk} will be studied using the same statistical linear model. Thus we present the model using a generic notation y_{ijk}.

To study the effects of the modality, the time duration and the serial order of tap in the trial, we consider the following heteroscedastic general linear model (*model* M_9), combining quantitative (interval time t^s) and qualitative factors (modality and serial order), which is written as:

$$y_{ijk} = \alpha + \alpha_j^1 + \alpha_k^2 + \alpha_{jk}^{12} + \left(\beta + \beta_j^1 + \beta_k^2 + \beta_{jk}^{12}\right)t_{ijk}^s + t_{ijk}^s\varepsilon_{ijk} \qquad (M_9)$$

$$\varepsilon_{ijk} \sim_{i.i.d} N(0, \sigma^2)$$

This model allows the combination of a linear regression (against the interval time) and an analysis of the effects of qualitative factors. In *model* M_9, α is the fixed effect, α_j^1 and β_j^1 model the effect of the serial order, α_k^2 and β_k^2 the effect of the modality, and α_{jk}^1 and β_{jk}^{12} their interaction.

Remark 1. The superiority of the heteroscedastic model (variance of the noise observation depending on t_{ijk}^s) over the homoscedastic one (constant noise variance) is widely supported by the literature. Indeed, it has been broadly demonstrated that the standard deviation increases linearly as a function of the interval, which is called the scalar property of interval timing (Gibbon et al. 1997; Ivry and Hazeltine 1995; Merchant et al. 2008b; see also Fig. 4*C*). That is why this structure of noise variance is adopted here.

In a standard factor analysis, each effect is removed one by one, and this new model is compared with the complete one (*model* M_9) using standard hypothesis testing. In this paper, we propose a more complete study, considering all the possible models (including any possible combination of the factors) and comparing globally using a

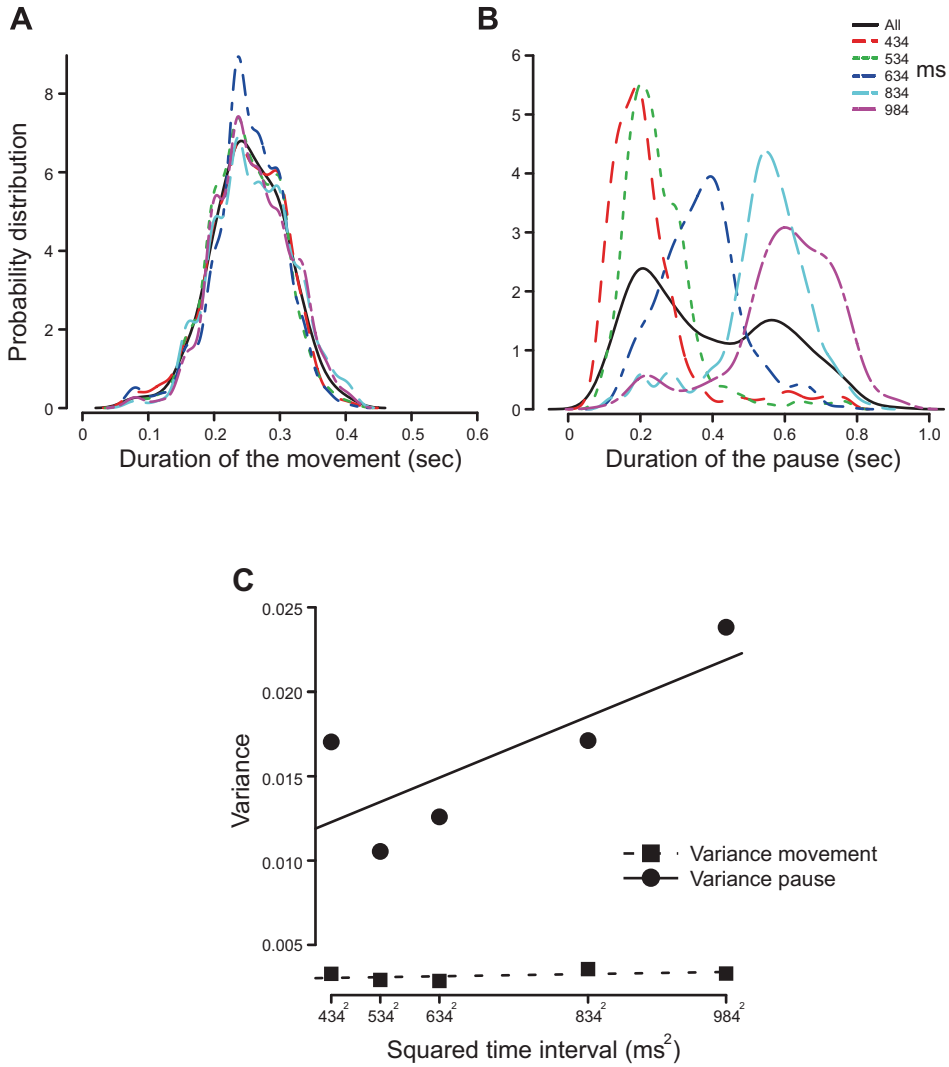

Fig. 4. Distribution of the movement (*A*) and pause (*B*) durations. Solid line (black): distribution for all the time durations. Dashed line (red): for durations equal to 434 ms. Dotted line (green): for durations equal to 534 ms. Dotted-dashed line (blue): for durations equal to 634 ms. Long dash line (cyan): for durations equal to 834 ms. Two dashed line (magenta): for durations equal to 984 ms. *C*: variance of the pause durations (dots) and the movement durations (squares) as functions of the time squared time interval $(ts)^2$ with linear regressions: the slope of the regression line for the pause variance is equal to 1.23×10^{-8}, whereas the slope of the regression line for the movement variance is equal to 4.52×10^{-10}.

model selection procedure. We now present the collection of models and discuss the model selection procedure.

Collection of models. Model M_9 is the most complete model we can suggest, including all the listed factors. In Table 1, we summarize the collection of submodels of *model M_9*, including or not the factors of interest, considering any possible combination of the factors. Since it would be fastidious to present the complete collection of models (16 in total), we give the following two examples and postpone the complete list to the APPENDIX A.

The simplest model is the one including no effects:

$$y_{ijk} = \alpha + t^s_{ijk}\varepsilon_{ijk}, \ \ \varepsilon_{ijk} \sim_{i.i.d} N(0, \sigma^2) \qquad (M_0)$$

To consider a conjoint effect of the time interval and of the modality, we define:

$$y_{ijk} = \alpha + \alpha^2_k + (\beta + \beta^2_k)t^s_{ijk} + t^s_{ijk}\varepsilon_{ijk}, \ \ \varepsilon_{ijk} \sim_{i.i.d} N(0, \sigma^2) \quad (M_3)$$

Besides, we are also interested in the effect of synchronization/continuation ($j = 1, 2, 3$ or $j = 4, 5, 6$) over the movement/pause. In this case, there is no sense in introducing a third variable, because this one would be included in the variable "serial order of the tap." So we resort to defining new submodels of the ones previously described. More precisely, for each model, including the variable "serial order of the tap" (e.g., *models M_4* to *M_9* in Table 1), we propose a new corresponding submodel such that:

$$\beta^1_1 = \beta^1_2 = \beta^1_3 \qquad \beta^1_4 = \beta^1_5 = \beta^1_6$$
$$\alpha^1_1 = \alpha^1_2 = \alpha^1_3 \qquad \alpha^1_4 = \alpha^1_5 = \alpha^1_6$$

leading to six more models, which are also listed in Table 1. Table 1 also specifies the number of parameters involved in each model.

Bayesian model selection for the heteroscedastic linear model. Model selection is a key issue in statistical inference. Assume that you have a set of data y and a collection of models $M_1,...,M_M$ in competition, each model being defined by a likelihood $l_m(y|\theta_m)$, depending on an unknown parameter θ_m of dimension d_m. We aim at defining a quantitative criteria to choose the model (among the given collection), which is the "most adapted" to the data y. In the Bayesian version of model selection, a prior probability is set on each model $p_m(M_m)$, and the models are compared through their posterior probability:

$$p_m(M_m|y) = \frac{p(y|M_m)p_m(M_m)}{p(y)}$$

where $p(y|M_m)$ is the marginal likelihood, equal to $p(y|M_m) = \int_{\theta_m} l_m(y|\theta_m)\pi_m(\theta_m)d\theta_m$, with $\pi_m(\theta_m)$ being the prior distribution of the parameters θ_m of model M_m. In the case of our heteroscedastic linear model, the posterior probability of each model can be computed in a closed form, provided a judicious choice of the prior distributions on the parameters. The details of the procedure are given in APPENDIX B.

Table 1. *Collection of tested models*

Model	Time Interval	Serial Order	Synchronization/ Continuation	Modality	Interaction of 1 and 2	No. of Parameters
M_0						2
M_1	X					3
M_2				X		3
M_3	X			X		5
M_4		X				7
M_5	X	X				13
M_6		X		X		8
M_7	X	X		X		15
M_8		X		X	X	13
M_9	X	X		X	X	25
M_{10}			X			3
M_{11}	X		X			5
M_{12}			X	X		4
M_{13}	X		X	X		7
M_{14}			X	X	X	5
M_{15}	X		X	X	X	9

Column 1, model index. The following columns show the absence or presence (X) of the various factors: *column 2*, time duration; *column 3*, serial order of the movement in the trial sequence; *column 4*, synchronization or continuation; *column 5*, modality (visual or auditory); *column 6*, interaction of the serial order or synchronization/continuation with the modality; *column 7*, corresponding number of parameters of the model.

RESULTS

Model Selection Procedure

We present in Tables 2–5, the results we obtained on the model selection for the two monkeys (considered individually or together), for the pause and the movement. For each monkey and each type of data (movement or pause), we give the list of the models ordered by decreasing $\log_{10}$ marginal likelihood. Note that this is equivalent to ordering them through their posterior probabilities, since we set uniform prior probabilities on the models. In the last columns of Tables 2–5, we compute the Bayes Factor (in $\log_{10}$ scale) for each consecutive pair of ordered models $M_{(m)}$ and $M_{(m+1)}$:

$$\log_{10} B_{m,m+1} = \log_{10} \frac{p\left(M_{(m)} \middle| y\right)}{p\left(M_{(m+1)} \middle| y\right)} = \log_{10} p\left(y \middle| M_{(m)}\right) - \log_{10} p\left(y \middle| M_{(m+1)}\right) \quad (1)$$

Since the models have been ordered, these quantities are negative. The $\log_{10}B_{m;m+1}$ can be interpreted with the Jeffrey scale of evidence, setting that if $|\log_{10}B_{m,m+1}| < 0.5$, the evidence for model $M_{(m)}$ is weak; if $0.5 < |\log_{10}B_{m,m+1}| < 1$, the evidence is substantial; if $1 < |\log_{10}B_{m,m+1}| < 2$, the evidence is strong; and if $2 < |\log_{10}B_{m,m+1}|$ the evidence is decisive.

Statistical Interpretation

On the pause. Table 2 gives the results of the model selection procedure for the pause duration for monkeys M01 and M02, separately, whereas Table 3 gives the model selection results using the data of monkeys M01 and M02 conjointly, but without introducing an additional effect of the monkey.

First of all, note that, from all tables, it is clear that the models involving an effect of the time duration (models with an odd index) are better than the ones which do not take that effect into account (models with an even index). In Table 3, the first ranked model ignoring the time duration effect (M_0) arrives after all the other models, including that effect and with a large Bayes Factor (-191.99 in favor of *model* M_9). The models including the time duration effects can be divided into two groups, namely, models $\{M_1, M_{11}, M_3, M_{13}, M_{15}\}$ and $\{M_5, M_7, M_9\}$, the two groups being separated by a large gap in the Bayes factor (-15 in Table 3). The models of the first group takes into account the effect of synchronization-continuation, whereas the other group includes the effect of the serial order of the tap. The model selection procedure clearly pleads in favor of a simpler model.

In Fig. 5, we plot the regression lines obtained for the two models of interest, namely *model* M_1, which only includes the effect of the time duration and is the best with respect to the Bayesian model selection procedure, and *model* M_{15} (which is

Table 2. *Results of the Bayesian model selection for the pause*

	Monkey M01			Monkey M02		
Rank	Model	$\log_{10}$ Marginal Likelihood	BF	Model	$\log_{10}$ Marginal Likelihood	BF
1	15	2437.23		1	2620.68	
2	1	2431.49	−5.74	3	2616.73	−3.94
3	11	2431.15	−0.34	11	2616.68	−0.05
4	3	2428.71	−2.43	13	2612.74	−3.94
5	13	2428.44	−0.28	15	2609.01	−3.73
6	5	2426.78	−1.66	5	2601.89	−7.12
7	7	2424.31	−2.47	7	2597.99	−3.91
8	9	2418.94	−5.37	9	2574.95	−23.04
9	0	2168.56	−250.38	0	2549.67	−25.28
10	2	2166.76	−1.81	10	2547.67	−1.99
11	10	2166.58	−0.18	2	2547.34	−0.34
12	12	2164.77	−1.81	12	2545.34	−1.99
13	14	2164.67	−0.1	14	2543.49	−1.85
14	4	2158.54	−6.13	4	2541.06	−2.43
15	6	2156.75	−1.8	6	2538.74	−2.33
16	8	2147.25	−9.5	8	2527.24	−11.49

Monkey M01 is shown on the *left*, and monkey M02 on the *right*. *Columns 2* and *5*, indexes of the ordered models. *Columns 3* and *6*, evaluated marginal likelihood (in $\log_{10}$). *Columns 4* and *7*: Bayes factors (BF) $\log_{10} B_{m,m+1}$ (*Eq. 1*).

Table 3. *Results of the Bayesian model selection for the pause, for monkeys M01 and M02 simultaneously*

	Monkeys M01 and M02		
Rank	Model	$\log_{10}$ Marginal Likelihood	BF
1	1	4942.78	
2	11	4940.67	−2.11
3	3	4939.86	−0.81
4	13	4937.76	−2.1
5	15	4937.76	0
6	5	4922.75	−15
7	7	4919.86	−2.89
8	9	4900.92	−18.94
9	0	4708.93	−191.99
10	10	4707.41	−1.52
11	2	4706.7	−9.71
12	12	4705.18	−1.52
13	14	4705.17	−0.01
14	4	4697.97	−7.2
15	6	4695.74	−2.23
16	8	4686.14	−9.6

Column 2, indexes of the ordered models. *Column 3*, evaluated marginal likelihood (in $\log_{10}$). *Column 4*, BF $\log_{10} B_{m,m+1}$ (*Eq. 1*).

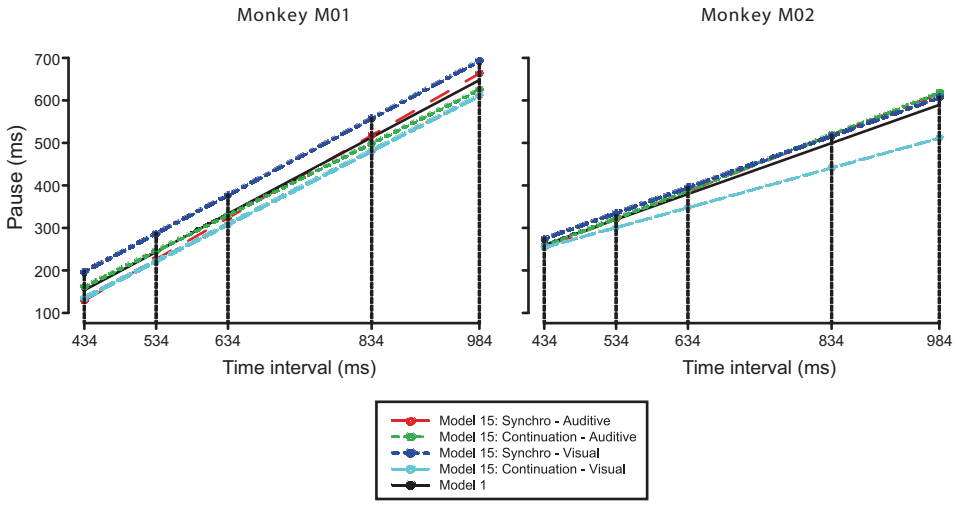

Fig. 5. Regression for monkeys M01 (*left*) and M02 (*right*) using *models M1* (plain black line) and *M15* (colored lines). For model *M15*, including the effects of synchronization-duration and the modality, the four regression lines are plotted, corresponding to the four groups of observation.

the most complete of the first group of models). The regression lines are given for monkeys M01 and M02 separately. In *model* M_{15}, the observed pauses are divided into four groups (*group 1*: auditory task of synchronization; *group 2*: auditory task of continuation; *group 3*: visual task of synchronization; *group 4*: visual task of continuation). A linear regression function is computed for each group of observation. These results support two important notions: first, that both monkeys controlled the pause-duration to correctly perform the SCT; and second, the pause-duration had an interaction with serial order.

On the movement. The results of the model selection procedure for the movement duration are given in Table 4 for monkeys M01 and M02, separately, and Table 5 for monkeys M01 and M02 conjointly. Contrary to the pause data, the four better models (obtained on monkeys M01 and M02 conjointly) in this case do not involve the effect of time duration. The phenomenon is quite similar when we study the monkeys individually. Moreover, we cannot highlight groups of models and so identify important variables, which could have a major effect in general on the duration of the movement.

Table 4. *Results of the Bayesian model selection for the movement*

	Monkey M01			Monkey M02		
Rank	Model	$\log_{10}$ Marginal Likelihood	BF	Model	$\log_{10}$ Marginal Likelihood	BF
1	4	2605.62		12	3060.48	
2	6	2603.12	−2.5	14	3058.09	−2.39
3	11	2602.96	−0.16	2	3055.38	−2.71
4	0	2600.75	−2.21	6	3055.37	−0.01
5	10	2600.67	−0.08	13	3053.85	−1.52
6	8	2600.22	−0.45	3	3051.12	−2.74
7	5	2599.82	−0.4	15	3048.98	−2.14
8	1	2599.22	−0.61	8	3045.56	−3.41
9	2	2598.26	−0.96	7	3039.72	−5.84
10	12	2598.17	−0.08	10	3035.69	−4.03
11	13	2597.97	−0.21	0	3031.6	−4.1
12	14	2597.93	−0.04	11	3030.94	−0.66
13	15	2595.66	−2.27	4	3029.92	−1.01
14	7	2594.83	−0.084	1	3029.24	−0.69
15	3	2594.22	−0.061	9	3017.93	−11.3
16	9	2580.98	−13.24	5	3016	−1.94

Monkey M01 is shown on the *left*, and monkey M02 on the *right*. *Columns 2* and *5*, indexes of the ordered models. *Columns 3* and *6*, evaluated marginal likelihood (in $\log_{10}$). *Columns 4* and *7*, BF $\log_{10} B_{m,m+1}$ (*Eq. 1*).

DISCUSSION

This study demonstrates that monkeys used an explicit timing mechanism to control the duration of their tapping pauses to execute properly the SCT. Our results also indicate that monkeys used a stereotyped motor command to perform the button-press movement. Furthermore, we used a model selection approach using Bayesian inference that shows the most important factor that explained the duration of the tapping pauses in the interval duration of the SCT, with the interaction between interval duration and the serial-order or task phase playing also some role.

The results on the analysis of the probability distributions confirmed the presence of the scalar property of interval timing in the temporal variability of the pause, but not the movement, duration in monkeys performing the SCT. In fact, 96% of the variability of the duration of a complete cycle (pause + movement) was due to the variability of the pause duration,

Table 5. *Results of the Bayesian model selection for the movement duration, for monkeys M01 and M02 simultaneously*

Rank	Model	Monkeys M01 and M02 $\log_{10}$ Marginal Likelihood	BF
1	12	5466.35	0
2	14	5464.79	−1.56
3	10	5464.67	−0.12
4	2	5463.36	−1.31
5	11	5462.13	−1.23
6	0	5461.74	−0.38
7	13	5461.42	−0.32
8	1	5459.75	−1.67
9	3	5458.95	−0.8
10	15	5457.41	−1.54
11	6	5457.39	−0.02
12	4	5455.7	−1.69
13	8	5449.47	−6.23
14	5	5443.33	−6.14
15	7	5442.64	−0.69
16	9	5422.48	−20.15

Column 2, indexes of the ordered models. *Column 3*, evaluated marginal likelihood (in $\log_{10}$). *Column 4*, BF $\log_{10} B_{m,m+1}$ (*Eq. 1*).

with the remaining being explained by a small variability of the movement (8% of the total variability) and a small negative covariation (−2%) between the pause and movement durations. This analysis was inspired by the classical Wing and Kristofferson model (1973) that assumed that the total variability in the SCT can be decomposed in the variability associated with a central timer and the variability of the motor implementation. Their model predicted a strict dependence between adjacent intervals, with a lag-one autocovariance that is equal to the negative variance of the motor implementation (Wing and Kristofferson 1973). Using this model, it is possible to compute indirectly the variance associated with the central timer, by calculating the total variance and the variance associated with the motor implementation that depends on the lag-one autocovariance. Thus many authors have demonstrated a linear increase in the variance of the central timer as a function of interval, while the variance of the motor implementation is constant across the produce intervals (Balasubramaniam et al. 2004; Ivry and Keele 1989; Wing 1980; see Wing 2002 for a review). In line with these observations, a recent study showed that transcranial magnetic stimulation in the motor cortex applied synchronously with the sensory metronome induced complex finger trajectories, but did not had an effect on the temporal performance on human subjects performing a synchronization tapping task (Levit-Binnun et al. 2007). Due to the kinematic analysis of the velocity of the tapping behavior, in the present paper we were able to directly quantify the duration of the pause and the motor execution, and our results demonstrate for the first time that only the pause follows the scalar property of interval timing (Gibbon et al. 1997). Consequently, our findings not only indicate that monkeys time their tapping behavior controlling the pause-duration by a timing mechanism, but also imply a direct validation of the Wing and Kristofferson model (1973), demonstrating that the total tapping variance of the SCT can be decomposed on the timing and motor variability, using the speed profile of the subject to directly quantify these measures (see Fig. 4).

In previous papers, our laboratory has demonstrated that Rhesus monkeys (*Macaca mulatta*) show some but not all of the behavioral traits that define rhythmic entrainment (Merchant et al. 2011; Merchant and Honing 2014; Zarco et al. 2009). Rhythmic entrainment refers to the ability to align motor actions with an auditory beat or pulse that marks equally spaced points in music or a sequence of auditory stimuli (Large and Palmer 2002; Merchant and Honing 2014), and for long has been considered a complex skill exclusive of humans and a selected group of bird species that show vocal learning (Honing et al. 2012; Patel 2006; Patel et al. 2009). Nevertheless, Rhesus monkeys show appropriate tempo matching during the SCT, with movement periods that slightly underestimated the sensory metronome periods (50 ms) for a range of intervals from 450 to 1,000 ms (Zarco et al. 2009). The present findings support these observations by the formal demonstration that monkeys have the ability to precisely time the duration of their movement pauses during the SCT. Furthermore, the pause-duration is by far the most important factor (compared with the serial order, the interval marker modality and the task phase) in the Bayesian model selection, and this behavioral parameter follows the scalar property of interval timing, a property that has been widely described in many timing tasks (Gibbon et al. 1997; Merchant et al. 2008b, 2008c, 2013a). On the other side, the monkeys' asynchronies (the time between the stimulus and the button press) are smaller during the SCT than their reaction times to stimuli with a random interonset interval (600–1,400 ms), indicating that these animals showed a predictive rhythmic behavior during the SCT (Zarco et al. 2009). The asynchronies in monkeys, however, are always lagging after the onset times of the metronome for 250 ms, which contrast with the negative mean asynchrony that is commonly found in humans (Repp 2005). Taken together, these observations indicate that, although Rhesus monkeys do not show the phase matching of humans, they show the remarkable ability to time their tapping pauses during a rhythmic behavior that is initially cued by a sensory metronome and then is internally driven.

The study of the movement trajectories during the SCT in humans has revealed two important properties: there is an asymmetry in the out and return phases of the movement trajectories (subjects made more rapid movements of shorter duration toward the temporal target and slower movements in the return phase), and the timed trajectories are less smooth and the spontaneous tapping movements, showing higher means squared jerk (Balasubramaniam et al. 2004). In addition, Doumas and Wing (2007) found that, although the movement trajectories changed as a function of interval during a SCT, the performance variability was largely attributable to the timing process rather than the motor process. In the present paper, we did not characterize the asymmetries in movement trajectories in monkeys; instead, we focused on the duration of the movement and the pauses using the speed profile of the trajectories to define these durations, and we found the timing control was largely exerted in the pause. Accordingly, it has been shown in humans performing an SCT tapping task that the holding period (pause or dwell) between flexion and extension increased as a function of the interval duration (Doumas and Wing 2007). However, that study did not perform a quantitative characterization of the pause of movement as in the present paper. Instead, cross-correlation analyses of the velocity of the finger flexion and extension across the produced intervals in a sequence showed that there was little dependence between interval timing and movement kinematics. As a hole, our findings and those obtained previously (Doumas and Wing 2007) suggest that the key element for timing control is the movement pause during the SCT, although changes in the movement trajectory can be performed for small adjustments or correction purposes.

In a series of psychophysical papers, Zelaznik and collaborators have suggested that explicit and implicit timing behavior can be dissociated (Robertson et al. 1999; Zelaznik et al. 2002, 2005). Classical explicit event timing tasks include the SCT, interval reproduction, and the discrimination and categorization of time intervals (Ivry and Hazeltine 1995), and performance in all of them follows the scalar property of interval timing (Merchant et al. 2008b). A key element in all these tasks is the phasic component of the perceived or executed durations, and different hypothesis have been delineated regarding its neural underpinnings (Buhusi and Meck 2005; Karmarkar and Buonomano 2007; Merchant et al. 2013a). In contrast, the continuous drawing task, where subjects constantly move their arm in synchrony with a sensory metronome or an internal cue, has been associated with an implicit timing process. Indeed, it has been suggested that the emergent temporalization of con-

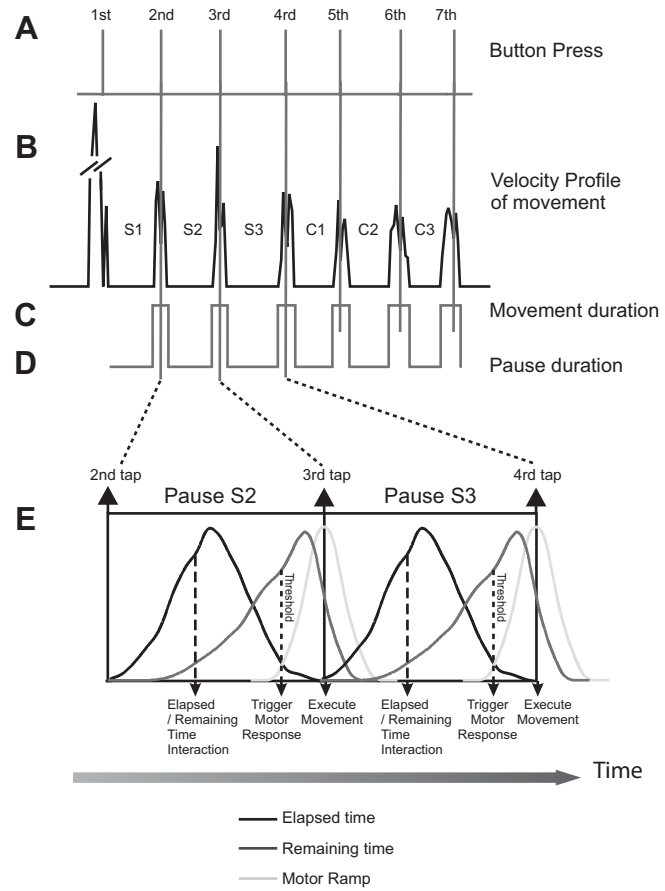

Fig. 6. A model of three ramping cell populations that control the pause duration and the execution of a ballistic cascade of movements associated with the stereotyped tapping behavior. *A*: times of the seven button presses recorded by the corresponding interphase. *B*: velocity profile of the movement extracted from the video recordings of the behaving monkeys. The thin vertical lines correspond to the times of button press, in accordance with *A*. *C* and *D*: movement and pause durations, respectively, directly computed from the velocity profile above. *E*: model that suggests that the tight interaction between the elapsed and remaining time ramping cells defined the pause duration. Once the remaining time cells reach a particular threshold in activity, they trigger the activity of the motor ramps that control of the fixed chain of movements engaged in a single stereotyped tapping behavior.

tinuous behaviors is not associated with a dedicated neural timing mechanism (Ivry et al. 2002; Spencer et al. 2003, 2007). The present kinematic observations demonstrate the phasic nature of the control that the monkeys exert on their tapping behavior during the SCT. Most of the movement variability is explained by the pause duration, whereas the movement execution is somehow stereotyped. Furthermore, previous electromyography measurements in different muscles of the forearm, arm, and shoulder of monkeys executing the SCT have corroborated the low variation of the movement and the phasic activation of the musculature of the tapping arm (Merchant et al. 2011). Finally, the Bayesian model selection indicated that, in contrast to the pause duration, the movement duration is not importantly affected by the interval, modality, or serial order of the SCT. Hence, our results support the idea that the timing mechanism engaged during the SCT triggers a fixed program that controls the downward movement, the button press, and the upward movement to get the hand in the pause position.

The explicit timing strategy used by the monkeys during the SCT can be simply explained by the interaction of three populations of ramping neurons in the medial premotor areas, previously described in our laboratory (Merchant et al. 2011). The instantaneous activity of these cells could encode: *1*) the elapsed time since the previous tap, by showing an up-down profile of activation whose duration changes as a function of the time passed; 2) the remaining time to the next tap, by showing a linear increase in activity that peaks at a particular time before the movement execution (independently of the interval duration); or *3*) the tapping movements, by showing the same profile of activation across the serial order and interval durations. Figure 6 shows the ramping activity of the three ramping cell types during the SCT. We suggest that the tight interaction between the elapsed and remaining time ramps define the pause duration of each element of the rhythmic sequence. Then, once the time-remaining cells reach a particular activity level, they trigger the motor ramps and the motor command involved in the control of the fixed chain of movements engaged in a single stereotyped tapping behavior. Finally, the corollary discharge of the tapping movement activates, again, the elapsed time-ramping cells in another rhythmic cycle of the SCT.

APPENDIX A: LIST OF THE STATISTICAL MODELS

In this Appendix section, we describe the complete collection of statistical models, starting from the simplest one.

M_0 is the simplest model, including no effect of any factor:

$$\beta = \beta_j^1 = \beta_k^2 = \beta_{jk}^{12} = \alpha_j^1 = \alpha_k^2 = \alpha_{jk}^{12} = 0$$
$$y_{ijk} = \alpha + t_{ijk}^s \varepsilon_{ijk},\ \varepsilon_{ijk} \sim N(0, \sigma^2) \qquad (M_0)$$

M_1 only takes into account the effect of the time interval t_{ijk}^s:

$$\beta_j^1 = \beta_k^2 = \beta_{jk}^{12} = \alpha_j^1 = \alpha_k^2 = \alpha_{jk}^{12} = 0$$
$$y_{ijk} = \alpha + \beta t_{ijk}^s + t_{ijk}^s \varepsilon_{ijk},\ \ \varepsilon_{ijk} \sim N(0, \sigma^2) \qquad (M_1)$$

M_2 includes the effect of the modality (visual or auditory):

$$\beta = \beta_j^1 = \beta_k^2 = \beta_{jk}^{12} = \alpha_j^1 = \alpha_{jk}^{12} = 0$$
$$y_{ijk} = \alpha + \alpha_k^2 + t_{ijk}^s \varepsilon_{ijk},\ \ \varepsilon_{ijk} \sim N(0, \sigma^2) \qquad (M_2)$$

In M_3, we consider a conjoint effect of the modality (visual or auditory) and of the time interval:

$$\beta_j^1 = \beta_{jk}^{12} = \alpha_j^1 = \alpha_{jk}^{12} = 0$$
$$y_{ijk} = \alpha + \alpha_k^2 + (\beta + \beta_k^2) t_{ijk}^s + t_{ijk}^s \varepsilon_{ijk},\ \ \varepsilon_{ijk} \sim N(0, \sigma^2) \qquad (M_3)$$

In M_4, we consider an effect of the serial order of the movement in the trial sequence (only):

$$\beta = \beta_j^1 = \beta_k^2 = \beta_{jk}^{12} = \alpha_k^2 = \alpha_{jk}^{12} = 0$$
$$y_{ijk} = \alpha + \alpha_j^1 + t_{ijk}^s \varepsilon_{ijk},\ \ \varepsilon_{ijk} \sim N(0, \sigma^2) \qquad (M_4)$$

In M_5, we take into account a conjoint effect of the serial order of the movement in the trial sequence and of the time interval:

$$\beta_k^2 = \beta_{jk}^{12} = \alpha_k^2 = \alpha_{jk}^{12} = 0$$
$$y_{ijk} = \alpha + \alpha_j^1 + (\beta + \beta_j^1) t_{ijk}^s + t_{ijk}^s \varepsilon_{ijk},\ \ \varepsilon_{ijk} \sim N(0, \sigma^2) \qquad (M_5)$$

In M_6, we consider an effect of the serial order of the movement in the trial sequence and of the modality (without interaction):

$$\beta = \beta_j^1 = \beta_k^2 = \beta_{jk}^{12} = \alpha_{jk}^{12} = 0$$

$$y_{ijk} = \alpha + \alpha_j^1 + \alpha_k^2 + t_{ijk}^s \varepsilon_{ijk}, \quad \varepsilon_{ijk} \sim N(0, \sigma^2) \qquad (M_6)$$

M_7 is like *model* M_6, but also takes into account the time interval (still without interaction between *variables 1* and *2*):

$$\beta_{jk}^{12} = \alpha_{jk}^{12} = 0$$
$$y_{ijk} = \alpha + \alpha_j^1 + \alpha_k^2 + (\beta + \beta_j^1 + \beta_k^2) t_{ijk}^s + \varepsilon_{ijk}, \quad \varepsilon_{ijk} \sim t_{ijk}^s N(0, \sigma^2) \qquad (M_7)$$

M_8 is the same as *model* M_6, but including and interaction between *variables 1* and *2*:

$$\beta = \beta_j^1 = \beta_k^2 = \beta_{jk}^{12} = 0$$
$$y_{ijk} = \alpha + \alpha_j^1 + \alpha_k^2 + \alpha_{jk}^{12} + t_{ijk}^s \varepsilon_{ijk}, \quad \varepsilon_{ijk} \sim N(0, \sigma^2) \qquad (M_8)$$

M_9 is the complete model (effect of the serial order of the movement in the trial sequence, of the time interval and of the modality, with interaction between *variables 1* and *2*) and has been given before.

Besides, we are also interested in the effect of synchronization/continuation ($j = 1, 2, 3$ or $j = 4, 5, 6$) over the movement. In this case, we cannot introduce a third variable because this one would be included in the variable "serial order of the movement." So we just want to define a new submodel of the ones previously described. Also previously, for each model, including the variable "serial order of the movement" (e.g., *models* M_4–M_9), we propose a new submodel such that

$$\beta_1^1 = \beta_2^1 = \beta_3^1 \quad \beta_4^1 = \beta_5^1 = \beta_6^1$$
$$\alpha_1^1 = \alpha_2^1 = \alpha_3^2 \quad \alpha_4^1 = \alpha_5^1 = \alpha_6^1$$

As a consequence, we add six submodels to our collection of models. The collection of models and their number of parameters are summarized in the Table 1.

APPENDIX B: BAYESIAN MODEL SELECTION

General Comments on Bayesian Model Selection

Model selection is a key issue in statistical inference. Assume that you have a set of data y and a collection of models $M_1,\ldots, M_M$ in competition. Each model is defined by a likelihood $l_m(y|\theta_m)$, depending on a set of unknown parameters θ_m of dimension d_m.

The principle of model selection is to set a quantitative criteria aimed at choosing (among the given collection) the model which is the "most adapted" to the data y. Of course, the term "most adapted" is controversial. However, intuitively, we agree that a good model selection criteria should ensure a balance between the goodness of fit (how the model fits the data) and the simplicity of the model (in general its number of parameters d_m). Indeed, any extremely complicated model can fit to any data, but, in this case, the parameters may have no sense. In classical statistical inference, the goodness of fit is generally quantified through the likelihood function approach. The most famous model selection criteria are the Akaike Information Criteria (AIC) and the Bayesian Information Criteria (BIC). Each of them attributes a score to the models, and this score is used to order the models. AIC or BIC scores are defined as follows:

$$AIC(M_m) = l_m(y \mid \hat{\theta}_m) - \log d_m, \quad BIC(M_m) = l_m(y \mid \hat{\theta}_m) - 0.5 d_m \log(n)$$

where n is the number of observations, d_m is the dimension of the parameters, and $\hat{\theta}_m$ is the maximum likelihood estimator of θ_m: $\hat{\theta}_m = \text{argmax}_{\theta_m} l_m(y|\theta_m)$. Both AIC or BIC encourage models with a good fit [high maximized likelihood $l_m(y|\hat{\theta}_m)$] but penalize the dimension of the model (d_m) in a different way.

Remark 2. Note that, when one wants to compare only two *models* M_m and $M_{m'}$, it is standard to propose a statistical hypothesis test relying on the likelihood ratio: $R = \dfrac{l_m(y|\hat{\theta}_m)}{l_{m'}(y|\hat{\theta}_{m'})}$. *Model* $M_{m'}$ will be rejected as soon as this ratio is greater than a threshold s_α, which depends not only on the level of the test α, but also on the respective dimensions of the *models* M_m and $M_{m'}$, d_m and $d_{m'}$. The idea is the same as for a full set of models: the chosen model will ensure a compromise between goodness of fit and simplicity.

Bayesian model selection (Marin and Robert 2007; Robert 2007) is the Bayesian alternative to classical model selection. As before, we consider a collection of models $M_1,\ldots,M_M$, with each *model* M_m being characterized by a likelihood function $l_m(y|\theta_m)$ and a set of parameters θ_m. In Bayesian inference, a prior distribution is set on the parameters θ_m: $\theta_m \sim \pi_m(\theta_m)$. For each *model* M_m, this prior distribution is updated into the posterior distribution $p_m(\theta_m|y)$. Thanks to the Bayes formula, $p_m(\theta_m|y) = \dfrac{l_m(y|\theta_m)\pi_m(\theta_m)}{p(y|M_m)}$ where $p(y|M_m)$ is the normalizing constant of the posterior distribution, also called the marginal likelihood and equal to $p(y|M_m) = \int_{\theta_m} l_m(y|\theta_m)\pi_m(\theta_m)d\theta_m$.

When it comes out to Bayesian model selection, a prior probability distribution is set on the collection of models $[p(M_m)]_{m=1\ldots M}$. In general, we consider a uniform prior probability on the models (meaning that we do not prefer any model a priori): $p(M_m) = \dfrac{1}{M}, \forall m = 1\ldots M$. As for the parameters, the prior probability of each model can be updated into a posterior probability, taking into account the data y. The posterior probability of each model is obtained through the Bayes formula:

$$p(M_m|y) = \frac{p(y|M_m)p(M_m)}{p(y)}$$

where $p(y)$ is the normalizing constant $p(y) = \sum_{m=1}^{M} p(y|M_m)p(M_m)$ and $p(y|M_m)$ is the marginal likelihood of *model* M_m. These posterior probabilities will be used as scores to rank the models. Note that, contrary to classical model selection, no penalty needs to be considered. Thanks to the integration over the prior distribution, the posterior probabilities automatically penalize models with a large number of parameters (Berger at al. 2001).

Remark 3. The comment on the automatic choice of the penalty is supported by the fact that (for regular models) one can prove that, as the number of observations tends to infinity, the marginal likelihood can be approximated by the BIC. Moreover, note that no asymptotic assumption is made in the Bayesian model selection framework: this point is an argument in favor of the Bayesian framework vs. the classical one.

Remark 4. Note that, to compare two models, M_m and $M_{m'}$, we will naturally compute the ratio of the posterior probabilities. This ratio, called Bayes factor, is expressed as:

$$B_{m,m'} = \frac{p(M_m \mid y)}{p(M_{m'} \mid y)} = \frac{p(y \mid M_m)p(M_m)}{p(y \mid M_{m'})p(M_{m'})} = \frac{p(y \mid M_m)}{p(y \mid M_{m'})}$$

Thus the Bayes factor is a likelihood ratio. However, whereas in the classical statistical inference the parameters are "eliminated" by maximization, in the case of the Bayes factor, they are eliminated by integrating them out into the marginal likelihood.

Bayesian Model Selection for the Heteroscedastic Linear Model

In the heteroscedastic linear model, the posterior probabilities can be computed in a close form [provided a judicious choice of $\pi_m(\theta_m)$], thanks to a rescaling of the data. The details are given hereafter. First, we transform our heteroscedastic linear model into a homoscedastic

linear model. Then we specify the parameters, set identifiability conditions and define the prior distributions. Finally, we derive explicit expressions for the posterior distribution and the marginal likelihood. Note that all the details are given for the complete model (M_9), with the calculus being exactly the same for the other models.

From hetereroscedatic to homoscedastic model. Provided a rescaling of the data with respect to t^s_{ijk}, the heteroscedastic model can be written as a standard linear model with constant noise variance σ^2:

$$\tilde{y}_{ijk} = \frac{y_{ijk}}{t^s_{ijk}} = \left(\alpha + \alpha^1_j + \alpha^2_k + \alpha^{12}_{jk}\right)\left(t^s_{ijk}\right)^{-1} + \left[\beta + \beta^1_j + \beta^2_k + \beta^{12}_{jk}\right] + \varepsilon_{ijk}$$

$$\varepsilon_{ijk} \sim_{i.i.d} N\left(0, \sigma^2\right)$$

Identifiability. The parameters of interest of the complete model (M_9) are $\theta = (\underline{\alpha}, \underline{\beta}, \sigma^2)$, where

$$\underline{\alpha} = \left[\alpha, \left(\alpha^1_j\right)_{j=1\ldots6}, \left(\alpha^2_k\right)_{k=1,2}, \left(\alpha^{12}_{jk}\right)_{j=1\ldots6,k=1,2}\right]$$

$$\underline{\beta} = \left[\beta, \left(\beta^1_j\right)_{j=1\ldots6}, \left(\beta^2_k\right)_{k=1,2}, \left(\beta^{12}_{jk}\right)_{j=1\ldots6,k=1,2}\right]$$

To ensure the identifiability of the parameters, we set the following conditions:

$$\alpha^1_1 = \beta^1_1 = \alpha^2_1 = \beta^2_1 = 0,\ \alpha^{12}_{1j} = \beta^{12}_{1j} = 0 \quad \forall\ j = 1 \ldots 6 \text{ and } \alpha^{12}_{21} = \beta^{12}_{21} = 0$$

Model M_9 has the following matricial form:

$$\tilde{y} = \left(X^0, X^{time}\right)\begin{pmatrix}\alpha^{\mathrm{T}} \\ \underline{\beta}^{\mathrm{T}}\end{pmatrix} + \sigma\varepsilon = X\mu + \sigma\varepsilon,\ \ \varepsilon \sim N\left(0, I_n\right)$$

where $\tilde{y} \in \Re^n$ denotes the collection of rescaled data $\tilde{y} = (\tilde{y}_{ijk})_{i=1\ldots n_{jk}, j=1\ldots6, k=1,2}$, x^T is the transposed of x. $\mu = \begin{pmatrix}\alpha^T \\ \underline{\beta}^T\end{pmatrix} \in \Re^p$ (with $p = 24$ for *model M_9*). X^0 and X^{time} are matrices with 12 columns, such that their respective lines l, corresponding to trial i, modality k and tap serial order j, are equal to:

$$X^0_{l,\bullet} = \left(t^s_{ijk}\right)^{-1} v \text{ and } X^{time}_{l,\bullet} = v$$

where $v = (1, I_{\{j=2\}}, I_{\{j=3\}}, I_{\{j=4\}}, I_{\{j=5\}}, I_{\{j=6\}}, I_{\{k=2\}}, I_{\{j=2,\ k=2\}}, I_{\{j=3,\ k=2\}}, I_{\{j=4,\ k=2\}}, I_{\{j=5,\ k=2\}}, I_{\{j=6,\ k=2\}})$ and $I_{\{\}}$ is the index function.

Prior distributions on $\theta = (\mu, \sigma^2)$. We consider the following standard conjugate Zellner prior distribution on $\theta = (\mu, \sigma^2)$:

$$\mu|\sigma^2, X \sim N\left(0_{\Re p}, c\sigma^2\left(X^TX\right)^{-1}\right),\ \sigma^2 \sim Inv\Gamma\left(a, b\right)$$

where $Inv\Gamma(a, b)$ is the Inverse Gamma distribution. Note that the imposed identifiability conditions ensure the existence of $(X^T X)^{-1}$. In our application, the hyper-parameters (a, b, c) are set as follows. c controls the influence of the prior in the prior: as c goes to infinity, the influence vanishes at rate $1/c$. Setting $c = 1$ corresponds to giving the same weight to the data and the prior. In our case, we set $c = 10{,}000$, corresponding to a diffuse prior distribution. a and b control the prior distribution of σ^2. We set $a = b = 0$, leading to an improper (noninformative) prior distribution on σ^2:$\pi(\sigma^2) \propto (\sigma^2)^{-1}$ (i.e., the prior distribution is not a probability distribution, but the posterior distribution is). The use of a noninformative prior in a model selection context is in general prohibited. However, this rule does not apply here, since σ^2 has the same role in all the models in competition.

Posterior distributions of $(\mu, \sigma^2|\tilde{y})$. From *model M_9* and using the conjugacy of the prior distribution, we get the following posterior distribution:

$$\mu \,\big|\, \sigma^2, X, \tilde{y} \sim N\left(m_{post}, \sum_{post}\right),\ \sigma^2 \sim Inv\ \Gamma\left(a_{post}, b_{post}\right)$$

with

$$m_{post} = \frac{c}{c+1}\hat{\mu},\ \sum_{post} = \frac{\sigma^2 c}{c+1}\left(X^TX\right)^{-1}$$

$$a_{post} = a + \frac{n}{2},\ b_{post} = b + \frac{s^2}{2} + \frac{1}{2\left(c+1\right)}\tilde{y}^2X\left(X^TX\right)^{-1}X^T\,\tilde{y}$$

where $\hat{\mu} = (X^T|X)^{-1}\ X^T\ \tilde{y}$ is the mean square estimator of μ, and s^2 is the residual variance (up to a constant): $s^2 = (\tilde{y} - X\hat{\mu})^T\ (\tilde{y} - X\hat{\mu})$ (Marin and Robert 2007).

Marginal likelihood. As exposed before, the Bayesian model selection procedure relies on the marginal likelihoods. In the special case of the linear model with the conjugate Zellner prior, we are able to compute explicitly this quantity (see Marin and Robert 2007):

$$p(\tilde{y}|M) = \frac{b^a}{\Gamma\left(a\right)}\frac{1}{\left(2\pi\right)^{\frac{n}{2}}\left(c+1\right)^{\frac{p}{2}}}\Gamma\left(\frac{n}{2}+a\right)\left(\frac{1}{2}\tilde{y}^T\,R^{-1}\tilde{y} + b\right)^{\frac{n}{2}+a}$$

where $R = I_n + cX^T\ (X^TX)^{-1}\ X^T$, and p is the size of μ.

ACKNOWLEDGMENTS

We thank Victor de Lafuente for fruitful comments on the manuscript. We also thank Raul Paulin, Leopoldo Gonzalez-Santos, and German Mendoza for technical assistance.

GRANTS

This study was supported by El Consejo Nacional de Ciencia y Tecnología (151223) and Programa de Apoyo a Proyectos de Investigación e Innovación Tecnológica (IN200511) grants to H. Merchant. This study was partially funded by Fondo Europeo de Desarrollo Regional (FEDER) through the Operational Program Competitiveness Factors-COMPETE and National Funds through Fundação para a Ciência e a Tecnologia (FCT)-Foundation for Science and Technology projects: FCOMP-01-0124-FEDER-022682 (FCT PEst-C/EEI/UI0127/2011), Incentivo/EEI/UI0127/2013, and Carnegie Mellon-Portugal Program (faculty exchange program).

DISCLOSURES

No conflicts of interest, financial or otherwise, are declared by the author(s).

AUTHOR CONTRIBUTIONS

Author contributions: S.D., R.B., J.M.F., J.P.S.C., and L.P. analyzed data; S.D., J.M.F., J.P.S.C., and H.M. interpreted results of experiments; S.D., J.M.F., and H.M. prepared figures; S.D. and H.M. drafted manuscript; S.D. and H.M. edited and revised manuscript; S.D., R.B., J.M.F., J.P.S.C., and H.M. approved final version of manuscript; R.B., L.P., and H.M. performed experiments; H.M. conception and design of research.

REFERENCES

Balasubramaniam R, Wing AM, Daffertshofer A. Keeping with the beat: movement trajectories contribute to movement timing. *Exp Brain Res* 159: 129–34, 2004.

Bartolo R, Prado L, Merchant H. Information processing in the primate basal ganglia during sensory guided and internally driven rhythmic tapping. *J Neurosci* 34: 3910–3923, 2014.

Berger JO, Pericchi LR, Ghosh JK, Samanta T, De Santis F, Berger JO, Pericchi LR. Objective Bayesian methods for model selection: introduction and comparison. *Lect Notes Monogr Ser* 135–207, 2001.

Buhusi CV, Meck WH. What makes us tick? Functional and neural mechanisms of interval timing. *Nat Rev Neurosci* 6: 755–765, 2005.

Diehl RL, Lotto AJ, Holt LL. Speech perception. *Annu Rev Psychol* 55: 149–179, 2004.

Doumas M, Wing AM. Timing and trajectory in rhythm production (Abstract). *J Exp Psychol Hum Percept Perform* 33: 442, 2007.

Dum RP, Strick PL. Spinal cord terminations of the medial wall motor areas in macaque monkeys. *J Neurosci* 16: 6513–6525, 1996.

Fernandes JM, Tafula S, Cunha JP. 3D-Video-fMRI: 3D motion tracking in a 3T MRI environment. In: *Image Analysis and Recognition. 8th Interna-*

tional Conference, ICIAR 2011, Burnaby, BC, Canada, June 2011, Proceedings, edited by M Kamel, A Campilho. Berlin: Springer, 2011, LNCS 6754, pt. II, p. 59–67.

Gibbon J, Malapani C, Dale CL, Gallistel C. Toward a neurobiology of temporal cognition: advances and challenges. *Curr Opin Neurobiol* 7: 170–184, 1997.

Honing H, Merchant H, Heden G, Prado LA, Bartolo R. Rhesus monkeys (*Macaca mulatta*) can detect rhythmic groups in music, but not the beat. *PLos One* 7: e51369, 2012.

Ivry R, Keele S. Timing functions of the cerebellum. *J Cogn Neurosci* 1: 136–152, 1989.

Ivry RB, Hazeltine RE. Perception and production of temporal intervals across a range of durations: evidence of a common timing mechanism. *J Exp Psychol Hum Percept Perform* 21: 3–18, 1995.

Ivry RB, Spencer RM, Zelaznik HN, Diedrichsen J. The cerebellum and event timing. *Ann N Y Acad Sci* 978: 302–317, 2002.

Janata P, Grafton ST. Swinging in the brain: shared neural substrates for behaviors related to sequencing and music. *Nat Neurosci* 6: 682–687, 2003.

Karmarkar UR, Buonomano DV. Timing in the absence of clocks: encoding time in neural network states. *Neuron* 53: 427–438, 2007.

Large EW, Palmer C. Perceiving temporal regularity in music. *Cogn Sci* 26: 1–37, 2002.

Levit-Binnun N, Handzy NZ, Peled A, Modai I, Moses E. Transcranial magnetic stimulation in a finger-tapping task separates motor from timing mechanisms and induces frequency doubling. *J Cogn Neurosci* 19: 721–733, 2007.

Marin JM, Robert C. *Bayesian Core: A Practical Approach to Computational Bayesian Statistics.* New York: Springer, 2007.

Merchant H, Georgopoulos AP. Neurophysiology of perceptual and motor aspects of interception. *J Neurophysiol* 95: 1–13, 2006.

Merchant H, Zarco W, Bartolo R, Prado L. The context of temporal processing is represented in the multidimensional relationships between timing tasks. *PLoS One* 3: e3169: 1–9, 2008a.

Merchant H, Zarco W, Prado L. Do we have a common mechanism for measuring time in the hundreds of milliseconds range? Evidence from multiple interval timing tasks. *J Neurophysiol* 99: 939–949, 2008b.

Merchant H, Luciana M, Hooper C, Majestic S, Tuite P. Interval timing and Parkinson's disease: heterogeneity in temporal performance. *Exp Brain Res* 184: 233–248, 2008c.

Merchant H, Zarco W, Prado L, Pérez O. Behavioral and neurophysiological aspects of target interception. *Adv Exp Med Biol* 629: 201–220, 2009.

Merchant H, Zarco W, Pérez O, Prado L, Bartolo R. Measuring time with multiple neural chronometers during a synchronization-continuation task. *Proc Natl Acad Sci U S A* 108: 19784–19789, 2011.

Merchant H, Harrington D, Meck WH. Neural basis of the perception and estimation of time. *Annu Rev Neurosci* 36: 313–336, 2013a.

Merchant H, Pérez O, Zarco W, Gámez J. Interval tuning in the primate medial premotor cortex as a general timing mechanism. *J Neurosci* 33: 9082–9096, 2013b.

Merchant H, Honing H. Are nonhuman primates capable of rhythmic entrainment? Evidence for the auditory timing dissociation hypothesis. *Front Neurosci* 7: 274, 2014.

Patel AD. Musical rhythm, linguistic rhythm, and human evolution. *Music Percept* 24: 99–104, 2006.

Patel AD, Iversen JR, Bregman MR, Schulz I. Experimental evidence for synchronization to a musical beat in a nonhuman animal. *Curr Biol* 19: 827–830, 2009.

Perez O, Kass R, Merchant H. Trial time warping to discriminate stimulus-related from movement-related neural activity. *J Neurosci Methods* 212: 203–210, 2013.

Phillips-Silver J, Trainor LJ. Hearing what the body feels: auditory encoding of rhythmic movement. *Cognition* 105: 533–546, 2007.

Repp BH. Sensorimotor synchronization: a review of the tapping literature. *Psychon Bull Rev* 12: 969–992, 2005.

Repp BH, Su YH. Sensorimotor synchronization: a review of recent research (2006–2012). *Psychon Bull Rev* 20: 403–452, 2013.

Robert CP. *The Bayesian choice. From Decision-Theoretic Foundations To Computational Implementation* (2nd Ed.). Springer Texts in Statistics. New York: Springer, 2007.

Robertson SD, Zelaznik HN, Lantero DA, Bojczyk KG, Spencer RM, Doffin JG, Schneidt T. Correlations for timing consistency among tapping and drawing tasks: evidence against a single timing process for motor control. *J Exp Psychol Hum Perfor* 25: 1316–1330, 1999.

Silverman BW. *Density Estimation for Statistics and Data Analysis.* London: Chapman & Hall/CRC Monographs on Statistics & Applied Probability, 1986.

Spencer RM, Zelaznik HN, Diedrichsen J, Ivry RB. Disrupted timing of discontinuous but not continuous movements by cerebellar lesions. *Science* 300: 1437–1439, 2003.

Spencer RM, Verstynen T, Brett M, Ivry R. Cerebellar activation during discrete and not continuous timed movements: an fMRI study. *Neuroimage* 36: 378–387, 2007.

Wing AM. Timing of movement phases of a repeated response. *J Mot Behav* 12: 113–124, 1980.

Wing AM. Voluntary timing and brain function: an information processing approach. *Brain Cogn* 48: 7–30, 2002.

Wing AM, Kristofferson AB. Response delays and the timing of discrete motor responses. *Percept Psychophys* 14: 5–12, 1973.

Zarco W, Merchant H, Prado L, Mendez JC. Subsecond timing in primates: comparison of interval production between human subjects and Rhesus monkeys. *J Neurophysiol* 102: 3191–3202, 2009.

Zelaznik HN, Spencer RM, Ivry RB. Dissociation of explicit and implicit timing in repetitive tapping and drawing movements. *J Exp Psychol Hum Percept Perform* 28: 575–588, 2002.

Zelaznik HN, Spencer RM, Ivry RB, Baria A, Bloom M, Dolansky L, Justice S, Patterson K, Whetter E. Timing variability in circle drawing and tapping: probing the relationship between event and emergent timing. *J Mot Behav* 37: 395–403, 2005.